Physical Properties of $CsSnM_3$ (M = Cl, Br, I): A First Principle Study

Hayatullah[a], G. Murtaza[b,*], S. Muhammad[a], S. Naeem[b], M.N. Khalid[b] and A. Manzar[a]
[a]Materials Modeling Lab, Department of Physics, Hazara University, Mansehra, Pakistan
[b]Department of Physics, Islamia College University, Peshawar, Pakistan

(Received November 13, 2012; in final form March 31, 2013)

First principle calculations are carried out to investigate the structural, electronic and optical properties of cubic perovskites $CsSnM_3$ (M = Cl, Br, I). The theoretically calculated lattice constants are found to be in good agreement with the experimentally measured values as compared to previous calculations. It is found that these perovskites are direct band gap semiconductors. The electrons densities reveal strong ionic bonding between Cs and halide cations while strong covalent bonding between Sn and halide cations. Optical properties of these compounds like real and imaginary parts of the dielectric functions, refractive indices, extinction coefficients, reflectivities, optical conductivities and absorption coefficients are calculated. The direct band gap nature and high absorption power of these compounds in the infrared, visible and ultraviolet energy range predicts that these perovskites can be used in optical and optoelectronic devices working in this range of the spectrum.

DOI: 10.12693/APhysPolA.124.102
PACS: 71.15.Mb, 71.22.+i, 71.15.Ap

1. Introduction

The family of perovskite crystals (ABX_3) is an interesting class of materials which exhibit many interesting physical properties such as high thermoelectric power, ferroelectricity, superconductivity, charge ordering, spin dependent transport, colossal magneto-resistance and the interplay of structural, magnetic and optical properties [1–3]. These materials are frequently used as sensor, substrates, catalytic electrode in fuel cells and are also promising candidates for optoelectronics [4]. A new application for the perovskites is found in hybrid organics–inorganics material which was used in thin-film field--effect transistors [5, 6].

The halide perovskites (ABX_3) are known to exhibit interesting structural, elastic, electronic and optical properties [7–9]. The cesium based compounds $CsSnM_3$ (M = Cl, Br, I) have some interesting optical and electrical properties e.g. $CsSnBr_3$ crystal is of quasi-metal type [10], while $CsSnCl_3$ crystal has dielectric properties. Moreover, these crystals are characterized to show several structural phase transitions. The $CsSnCl_3$ crystals have a high-temperature transition from the monoclinic to the cubic phase at 390 K. This structural phase transition is non-uniform throughout the volume of the crystal, and the monoclinic and the cubic phases can coexist [11]. $CsSnBr_3$ was found by Clark et al. to undergo a semimetal–semiconductor phase transition [10]. Donaldson et al. observed, using the Mössbauer spectroscopy, that $CsSnBr_3$ has a cubic perovskite structure at room temperature and an anomalously low *s*-electron density at the Sn nucleus [12, 13]. The structural and electronic properties of $CsSnBr_3$ are experimentally and theoretically investigated [14–19], while no work yet published on the bonding and optical nature of this important compound except of Brik [20]. Therefore these properties are important to reinvestigate.

An early study on the structural information of $CsSnI_3$ compound in form of powders was reported by Scaife et al. [21]. A few years later, a yellow, needle-like $CsSnI_3$ microcrystal was synthesized and its crystal structure was independently studied by Mauersberger and Huber [22]. No additional information was available until the discovery of another polymorph of this compound by Yamada et al. [23] and they studied its phase transitions with temperature. Theoretically Chabot et al. studied the structural and electronic properties of $CsSnI_3$ polymorphs under pressure, however still no work was published on the optical properties of the compound [24]. Chung et al. also investigated the electronic and optical band gap nature of $CsSnI_3$ polymorph [25]. However in the cubic phase the details concerning the bonding and optical properties are still lacking.

In the present study we have reported the structural, electronic and optical properties of cubic perovskites $CsSnCl_3$, $CsSnBr_3$, and $CsSnI_3$. This study will cover the lack of theoretical data on these perovskites.

2. Computational details

In the present density functional calculations, full potential linearized augmented plane wave (FP-LAPW) method within the Wu–Cohen generalized gradient approximation (GGA) [26] as utilized in the Wien2k package [27], is used to solve Kohn–Sham equation [28] for the evaluation of the structural, elastic, electronic and optical properties of the compounds. In the full-potential scheme

*corresponding author; e-mail: murtaza@icp.edu.pk

the potential is of general shape. The core electrons are treated fully relativistically and the valence electrons are treated semirelativistically. R_{MT} value of 2.5, 2.5, 2.5, 2.5, and 2.07 a.u. is used for Cs, Sn, Cl, Br, and I respectively. For wave function in the interstitial region the plane wave cut-off value of $K_{\max} = 7/R_{\mathrm{MT}}$ is chosen. For the k-space integration in the irreducible Brillouin zone (IBZ), modified tetrahedron method [29] 165 k-points is used to obtain self-consistency for the calculations of electronic and optoelectronic properties using a denser mesh of 5000 k-points in the IBZ.

3. Results and discussion

3.1. Structural properties

The determination of structural parameters is necessary to account a material's structural behavior. Here, volume of the unit cell of each $CsSnM_3$ (M = Cl, Br, I) is optimized to obtain structural parameters like lattice constant, a [Å], bulk moduli, B [GPa], and its pressure derivative, B'. In the optimization procedure, the total energy of the unit cells for each compound is calculated by varying the unit cell volumes and plotted against corresponding energies using the Birch–Murnaghan's equation of state [30].

The optimization curves for the compounds are shown in Fig. 1. The ground state energy (E_0) is the minimum energy of the unit cell and the volume corresponding to this optimum energy is known as the ground state volume. In the ground state a, B, and B' are evaluated.

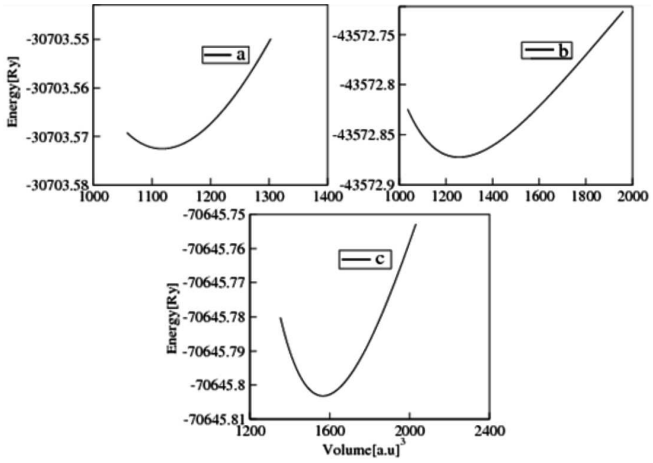

Fig. 1. Variation of total energy as a function of unit cell volume for $CsSnCl_3$ (a), $CsSnBr_3$ (b), and $CsSnI_3$ (c).

The calculated values of these parameters are compared with the available theoretical and experimental results in Table I. a increases as we go from Cl to Br to I. This increase in a is attributed to the increasing atomic size of the anions from Cl to Br to I. Our calculated values of a [Å] for $CsSnBr_3$ and $CsSnI_3$ are in good agreement with the available experimental results [17, 23]

TABLE I

Calculated lattice constants a_0 [Å], bulk moduli B [GPa], its pressure derivative B' and total ground state energy E_0 [Ry] for $CsSnM_3$ (M = Cl, Br, I) compared with other theoretical and experimental results.

	a_0	B	B'	E_0
$CsSnCl_3$				
this work	5.4901	27.68	3.81	−30703.5
other work	5.6537[a]	–	–	–
experiment	–	–	–	–
$CsSnBr_3$				
this work	5.7092	25.19	4.67	−43572.1
other work	5.565[a]	–	–	–
experiment	5.804[b]	–	–	–
$CsSnI_3$				
this work	6.1439	17.59	4.75	−70645.8
other work	5.930[a]	–	–	–
experiment	6.219[c]	–	–	–

[a]Ref. [18], [b]Ref. [17], [c]Ref. [23]

as compared to the previous calculation [18]. a [Å] for $CsSnCl_3$ are in good agreement with the theoretical calculated value by Verma et al. [18]. To the date no experimental value of a [Å] in cubic phase for $CsSnCl_3$ is available for comparison. B decreases from Cl to Br to I, which shows that compressibility and hardness of the material decreases with the change of anions. B' increases from Cl to I while E_0 is decreasing.

3.2. Electronic properties

The electronic nature of $CsSnM_3$ (M = Cl, Br, I) can be described in terms of band structure and density of states. The band structures for $CsSnM_3$ (M = Cl, Br, I) is shown in Fig. 2. The conduction band minimum and valence band maximum are located at the R symmetry point, hence these compounds are direct band gap materials. Direct band gaps in these compounds can also be seen at other symmetry points (M, Γ and X).

The fundamental band gaps at R and other symmetry points along with other theoretical results are presented in Table II. It can be seen from the table that band gaps decrease in going from Cl to Br to I. This decrease in the energy gap can be attributed to the fact that the conduction bands shift towards the Fermi level (E_{F}) when we move from Cl to Br to I. The overall reduction in the energy band gap is consistent with an overall weakening of the bonds, and therefore with a smaller bonding antibonding splitting.

Figure 2 also shows that along with conduction band, valence band at other symmetry points than R and lower valence bands are shifted towards the Fermi level as we go from Cl to Br to I. This fact is due to the increasing number of electrons in the respective bands and the occupancy of states near the Fermi level. The decreasing trend of band gaps by changing the anions from Cl to Br to I is also in agreement to the experimental and theoretical study of isoelectronic compounds $CsGeX_3$

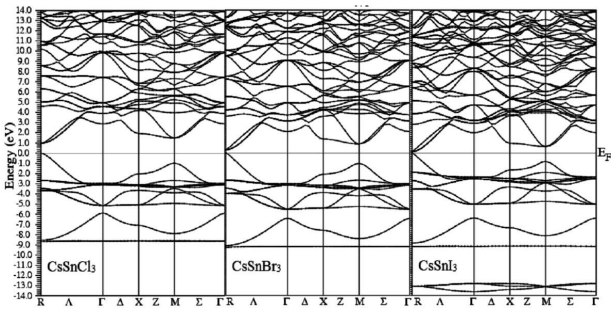

Fig. 2. Electronic band structure for $CsSnM_3$ (M = Cl, Br, I) in the high symmetry direction.

TABLE II

Band gap of $CsSnM_3$ (M = Cl, Br, I) at different symmetry points compared with experimental and other theoretical results in eV.

	$E_g^{R\text{-}R}$	$E_g^{M\text{-}M}$	$E_g^{X\text{-}X}$	$E_g^{\Gamma\text{-}\Gamma}$
$CsSnCl_3$				
this work	0.99	2.4	3.95	5
other work	–	–	–	–
$CsSnBr_3$				
this work	0.3	1.8	3.21	5.1
other work	0.42[a], 0.58[b], 0.35[c]	2.09[c]	3.45[c]	–
$CsSnI_3$				
this work	0.15	1.2	1.65	4.39
other work	0.434[d], 0.218[e]	–	–	–

[a]Ref. [17], [b]Ref. [14], [c]Ref. [20], [d]Ref. [24], [e]Ref. [35]

(X = Cl, Br) [31]. Our calculation shows $CsSnBr_3$ to be a narrow band gap semiconductor, which agrees with the theoretical calculation by Rose et al. [14] but is different from the calculations by Perry et al. [32] and Lefebvre et al. [15]. Using empirical tight-binding calculations, Perry et al. found the compound to be semimetallic, whereas Lefebvre et al. predict it to be a zero-gap semiconductor. The semiconducting nature with small band gap for the compound has also been predicted by Zheng et al. [33]. As a result the cubic phase of $CsSnBr_3$ should be semiconducting rather than semimetallic. The calculated value of energy gap for $CsSnBr_3$ and $CsSnI_3$ are in good agreement with the available theoretical results. To the date no experimental and theoretical value is available for comparison in $CsSnCl_3$ in cubic phase.

The electronic band gap nature can be further elucidated by the density of states. The total and partial densities of states for $CsSnM_3$ (M = Cl, Br, I) are presented in Figs. 3 and 4. The overall feature of total density of states (TDOS) remains the same in the three compounds. However, by changing the cations from Cl to Br to I, bands below valence and conduction bands are shifted towards the Fermi level. On the basis of different bands in the range −30 eV to 20 eV, TDOS could be grouped into four regions in $CsSnCl_3$, $CsSnBr_3$ and three regions in $CsSnI_3$.

The contributions of different states in these bands are shown in Fig. 4. The first region comprises on Sn d state in $CsSnCl_3$ and $CsSnBr_3$ while I s state in $CsSnI_3$, respectively. The second region in $CsSnCl_3$ and $CsSnBr_3$

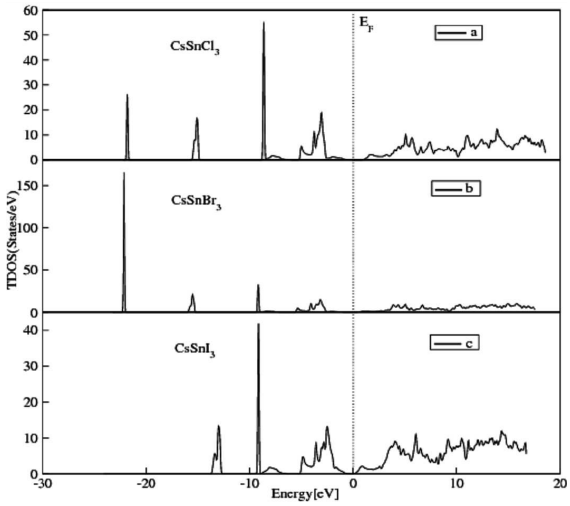

Fig. 3. Total density of states for $CsPbCl_3$ (a), $CsPbBr_3$ (b), and $CsPbI_3$ (c).

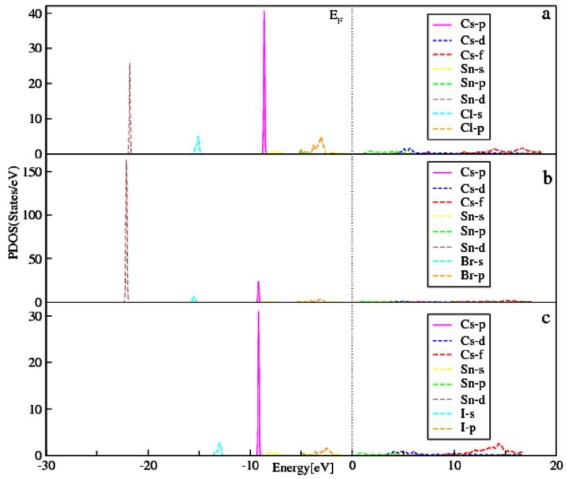

Fig. 4. Partial density of states for $CsPbCl_3$ (a), $CsPbBr_3$ (b), and $CsPbI_3$ (c).

is due to Cl s and Br s respectively while mixed Cs p and I p states in $CsSnI_3$. The third region (upper part) of the valence band in $CsSnCl_3$, $CsSnBr_3$ is due to Cs p and Cl p, Br p and I p and small portion of Sn s states, respectively. Fourth region in $CsSnCl_3$, $CsSnBr_3$, and third region in $CsSnCl_3$ after the Fermi level is the conduction band (CB). The lower part of this band near the Fermi level is mainly due to the Sn p state. Intermediate part is due to mixed states of Cs d and Sn p states. The upper part of this band is because of Cs f state.

The electronic charge density calculated by the first principle approach can be used to describe the bonding nature of the solids [34]. Charge densities for $CsSnM_3$ (M = Cl, Br, I) are calculated in the (1 0 0) and (1 1 0) planes and are shown in Fig. 5. Charge distribution in the (1 0 0) plane for $CsSnCl_3$, $CsSnBr_3$, and $CsSnI_3$ shows that the bonding between Cs–halide ions is strongly ionic

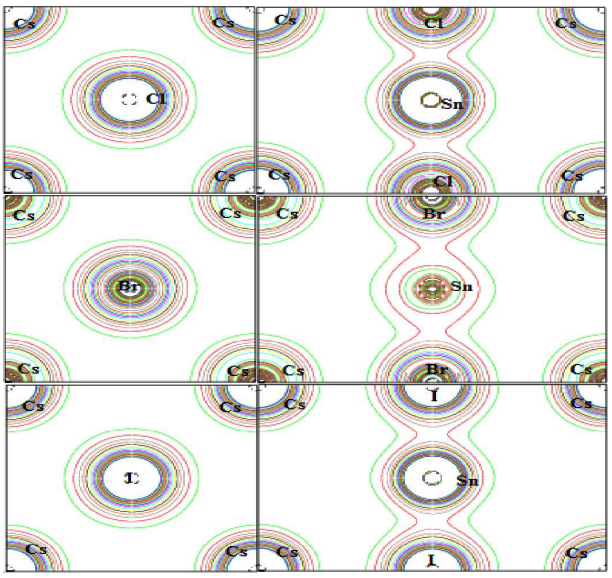

Fig. 5. Total electronic charge density for $CsSnCl_3$ (top), $CsSnBr_3$ (middle), and $CsSnI_3$ (bottom); right — the (1 0 0) plane and left — the (1 1 0) plane.

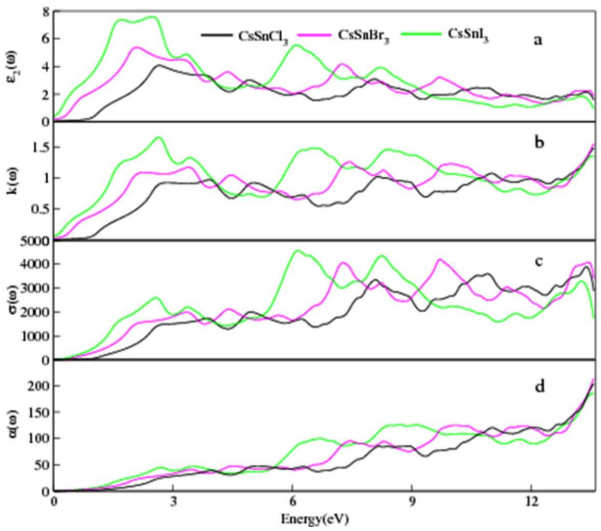

Fig. 6. Imaginary part of dielectric function (a), extinction coefficient (b), optical conductivity (c), and absorption coefficient (d) as functions of energy.

and this ionic nature enhances as we move from Cl to I in $CsSnM_3$. The density contours in (1 1 0) plane reveal that the bond between Sn and halogen ions (Sn–halide ions) is strongly covalent. The covalent nature of Sn–halide weakens and ionic nature slightly increases as we go from Cl to I in $CsSnM_3$. The covalent nature is mainly due to the hybridization of Sn p and Cs d states as clear from the PDOS (Fig. 4). Identical behavior has been seen for other calculations on $CsSnBr_3$ by Brik [20]. Similar behavior about the chemical bonding nature of $CsPbCl_3$, $CsPbBr_3$ and $CsPbI_3$ has also been reported in Ref. [7].

3.3. Optical properties

The complex dielectric function describes the complete response of a material to the disturbances caused by the electromagnetic radiations. The imaginary part of this function, $\varepsilon_2(\omega)$, is directly related to the band structure of the material and describes its absorptive behavior. From Fig. 6a, it can be seen that the spectra of $\varepsilon_2(\omega)$ for $CsSnM_3$ (M = Cl, Br, I) have similar features; however the absorption peaks are sharper and have higher magnitude for $CsSnI_3$ as compared to other two compounds. It is because of the narrower width of VB (Fig. 3) in $CsSnI_3$ as compared to the other two compounds. The critical points in the spectra of $\varepsilon_2(\omega)$ are found at 0.44, 0.19, and 0.046 eV for $CsSnCl_3$, $CsSnBr_3$ and $CsSnI_3$, respectively. Broad spectra of the dielectric function show high absorption in different regions of the energy spectrum. Similar features are found in the spectra (Fig. 6b) of the extinction coefficients, $k(\omega)$.

The optical conductivity spectra, $\sigma(\omega)$, presented in Fig. 6c show that optical conductance starts around 0.80, 0.29, and 0.18 eV for $CsSnCl_3$, $CsSnBr_3$, and $CsSnI_3$, respectively. Beyond these points $\sigma(\omega)$ increases and reaches there maxima and then again decreases and eventually dissipates with small variations. The $\sigma(\omega)$ is largest in $CsSnI_3$ as compared to the other two compounds. The highest value of conductivity is 3920.46 (13.36 eV), 4208.63 (9.72 eV) and 4568.34 (6.13 eV) for $CsSnCl_3$, $CsSnBr_3$, and $CsSnI_3$, respectively. Similar features are also observed for the absorption coefficients, $\alpha(\omega)$, Fig. 6d.

The frequency dependent real part of dielectric function, $\varepsilon_1(\omega)$, is shown in Fig. 7a. In the spectra the most important quantity is the zero frequency limit $\varepsilon_1(0)$, which is the electronic part of the static dielectric constant. Our calculated $\varepsilon_1(0)$ for $CsSnM_3$ (M = Cl, Br, I) are presented in Table III. From the table it is clear that $\varepsilon_1(\omega)$ increases in going from Cl to Br to I. This shows the inverse relation between the band gap and $\varepsilon_1(\omega)$. The $\varepsilon_1(0)$ for $CsSnBr_3$ is 7.491 which is in excellent agreement to the previous predicted value of 7 for this compound by Brik [20]. The $\varepsilon_1(0)$ for these compounds starts increasing from zero frequency limit, reaches its maximum value, then decreases, and in certain energy ranges it goes below zero. In these ranges the incident photon beam is completely attenuated.

The frequency dependent reflectivity $R(\omega)$ for these compounds is shown in Fig. 7b, while the zero frequency reflectivities are presented in Table III. It is noted that $R(0)$ also increases like $\varepsilon_1(\omega)$ with the change of cation from Cl to Br to I in $CsSnM_3$. Interestingly the maximum reflectivity occurs where $\varepsilon_1(\omega)$ goes below zero, which can be clearly seen in Fig. 7a,b. For negative values of $\varepsilon_1(\omega)$ the material shows metallic nature [36]. Reflectivity increases with metallicity of a compound and hence it is maximum for the range in which $\varepsilon_1(\omega)$ is negative. The reflectivity starts from 14% and reaches maximum

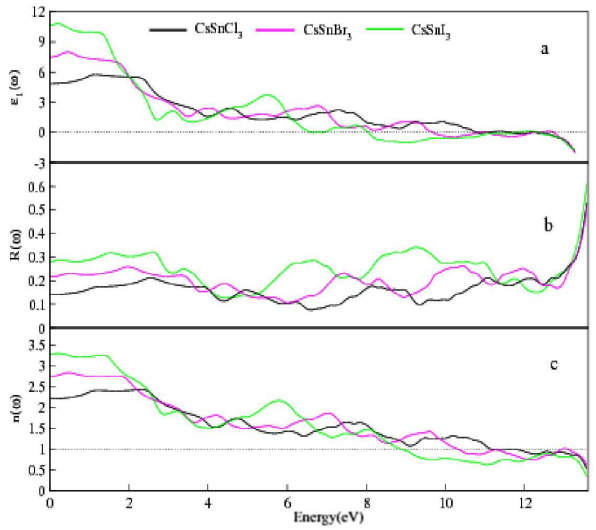

Fig. 7. Real part of dielectric function (a), reflectivity (b), and refractive index (c) as functions of energy.

TABLE III

Zero frequency limits of real part dielectric function, reflectivity and refractive index.

Parameters	$CsSnCl_3$	$CsSnBr_3$	$CsSnI_3$
$\varepsilon_1(0)$			
this work	4.14	7.491	10.615
other work	–	7.0[a]	–
$R(0)$			
this work	0.145	0.216	0.271
other work	–	–	–
$n(0)$			
this work	2.194	2.769	3.302
other work	–	–	–

[a]Ref. [20].

value of 52% for $CsSnCl_3$, while for $CsSnBr_3$ it starts from 21% and goes up to 51%. Similarly for $CsSnI_3$ it starts from 27% and reaches maximum value of 60%. So, the maximum reflectivity peak decreases in going from Cl to Br to I.

The knowledge of the refractive index of an optical material is important for its use in optical devices such as photonic crystals, waveguides, solar cells, and detectors. Figure 7c displays the variation in the refractive indices for $CsSnM_3$ (M = Cl, Br, I) as a function of incident photon energy. The data presented in Table III show that the calculated $n(0)$ increases from Cl to I. It is clear from Fig. 7c that the refractive indices of these materials increase from zero frequency limits and reach the maximum values of 2.45 for $CsSnCl_3$, 2.85 for $CsSnBr_3$ and 3.32 for $CsSnI_3$. The refractive index for each compound starts decreasing beyond maximum value and goes below unity in certain energy ranges. Refractive index lesser than unity ($v_s = c/n$) shows that the phase velocity of the incident radiation is greater than c.

4. Summary

The structural, electronic, and optical properties of $CsSnM_3$ (M = Cl, Br, I) are calculated by FP-LAPW method within the GGA. It is concluded that: As the halide ion changed from Cl to I in $CsPbM_3$ lattice constant and ground state unit cell energy increases, bulk modulus decrease and its derivative with pressure remains constant (5.0). It is found that these compounds have direct and wide band gap. The fundamental band gap occurs at R symmetry points which decrease in going from Cl to I. The strong ionic nature of Cs–halide bonds increases, and covalent nature in Sn–halide bonds decreases as cation change from Cl to I. The different structures appears in the spectra of the imaginary part of dielectric function mainly due to transitions from Cs and halide ions p states from the VB to unoccupied states in the CB. The zero frequency limits of dielectric function, reflectivity and refractive index increases from Cl to Br to I. The direct band gaps and high absorption power in the infrared, visible and ultraviolet energy range predicts the effective use of these compounds in the optical and optoelectronic devices, working in this range of the spectrum.

References

[1] N. Mathur, P. Littlewood, *Phys. Today* **56**, 25 (2003).

[2] S. Moskvin, A.A. Makhnev, L.V. Nomerovannaya, N.N. Loshkareva, A.M. Balbashov, *Phys. Rev. B* **82**, 035106 (2010).

[3] C. Weeks, M. Franz, *Phys. Rev. B* **82**, 085310 (2010).

[4] G. Murtaza, Iftikhar Ahmad, B. Amin, A. Afaq, M. Maqbool, J. Maqssod, I. Khan, M. Zahid, *Opt. Mater.* **33**, 553 (2011).

[5] C.R. Kagan, D.B. Mitzi, C.D. Dimitrakopoulos, *Science* **286**, 945 (1999).

[6] H. Klauk, *Phys. World* **13**, 18 (2000).

[7] G. Murtaza, Iftikhar Ahmad, *Physica B* **406**, 3222 (2011).

[8] G. Murtaza, Iftikhar Ahmad, M. Maqbool, H.A. Rahnamaye Aliabad, A. Afaq, *Chin. Phys. Lett.* **28**, 117803 (2011).

[9] B. Ghebouli, M.A. Ghebouli, M. Fatmi, A. Bouhemodou, *Solid State Commun.* **150**, 1896 (2010).

[10] S. Clark, C. Flint, J. Donaldson, *Phys. Chem. Solids* **42**, 133 (1981).

[11] A.S. Voloshinovskii, S.V. Myagkota, N.S. Pidzyrailo, M.V. Tokarivskii, *J. Appl. Spectr.* **60**, 226 (1994).

[12] J.D. Donaldson, R.M.A. Grimsey, S.J. Clark, *J. Phys. (France)* **40**, 289 (1979).

[13] J.D. Donaldson, J. Silver, S. Hadjeminolis, S.D. Ross, *J. Chem. Soc. Dalton*, 1503 (1975).

[14] S.K. Rose, S. Satpathy, O. Jepsen, *Phys. Rev. B* **47**, 4276 (1993).

[15] I. Lefebvre, P.E. Lippens, M. Lannoo, G. Allan, *Phys. Rev. B* **42**, 9174 (1990).

[16] D.E. Parry, M.J. Tricker, J.D. Donaldson, *J. Solid State Chem.* **28**, 401 (1979).

[17] J.C. Zheng, A.C.H. Huan, A.T.S. Wee, M.H. Kuok, *Surf. Interface Anal.* **28**, 81 (1999).

[18] A.S. Verma, A. Kumar, S.R. Bhardwaj, *Phys. Status Solidi B* **245**, 1520 (2008).

[19] K. Shum, Z. Chen, J. Qureshi, C. Yu Jian, J. Wang, W. Pfenninger, N. Vockic, J. Midgley, J.T. Kenney, *Appl. Phys. Lett.* **96**, 221903 (2010).

[20] M.G. Brik, *Solid State Commun.* **151**, 1733 (2011).

[21] D. Scaife, P. Weller, W. Fisher, *J. Solid State Chem.* **9**, 308 (1974).

[22] P. Mauersberger, F. Huber, *Acta Crystallogr. B* **36**, 683 (1980).

[23] K. Yamada, S. Funabiki, H. Horimoto, T. Matsui, T. Okuda, S. Ichiba, *Chem. Lett.* **20**, 801 (1991).

[24] J.F. Chabot, M. Côté, J.F. Brière, *APS Meeting Abstracts*, Vol. 1, 2004, p. 11011.

[25] I. Chung, J.H. Song, J. Im, J. Androulakis, C.D. Malliakas, H. Li, A.J. Freeman, J.T. Kenney, M.G. Kanatzidis, *J. Am. Chem. Soc.* **134**, 8579 (2012).

[26] Z. Wu, R.E. Cohen, *Phys. Rev. B* **73**, 235116 (2006).

[27] P. Blaha, K. Schwarz, G. Madson, D. Kvasnicka, J. Luitz, *User's Guide, WIEN2k*, Vienna University of Technology Austria (2002).

[28] W. Kohn, L.J. Sham, *Phys. Rev.* **140**, A1133 (1965).

[29] J.L. Erskine, E.A. Stern, *Phys. Rev. Lett.* **30**, 1329 (1973).

[30] F. Birch, *Phys. Rev.* **71**, 809 (1947).

[31] D.K. Seo, N. Gupta, M.H. Whangbo, H. Hillebrecht, G. Thiele, *Inorg. Chem.* **37**, 407 (1998).

[32] D.E. Parry, M.J. Tricker, J.D. Donaldson, *J. Solid State Chem.* **28**, 401 (1979).

[33] J.C. Zheng, C.H.A. Huan, A.T.S. Wee, M.H. Kuok, *Surf. Interface Anal.* **28**, 81 (1999).

[34] H. Jin, J. Im, A.J. Freeman, *Phys. Rev. B* **86**, 121102 (2012).

[35] R. Hoffman, *Rev. Mod. Phys.* **60**, 801 (1988).

[36] B. Xu, X. Li, J. Sun, L. Yi, *Eur. Phys. J. B* **66**, 483 (2008).